In Proceedings of IEEE International Conference on Robotics and Biomimetics (ROBIO '17), Macau, China (2017).

# Identifying invariant gait metrics for exoskeleton assistance

Graham Henderson, Daniel Gordon and Sethu Vijayakumar

***Abstract*— Exoskeletons have the potential to increase the independence and quality of life of patients with walking pathologies. To do this effectively, the exoskeleton requires a control paradigm that can determine the timing and magnitude of assistance that is suitable for the user's task and environment. This paper searches for a metric that can be optimised, enabling assistance to be applied without compromising the energy efficiency and stability of gait. Spatial and temporal, kinematic, kinetic, and other novel dynamic stability metrics were compared across three different assistance scenarios and five different walking contexts. Results demonstrated that three metrics: step width, medial-lateral centre of pressure displacement, and medial-lateral margin of stability were the most invariant. This result suggests dynamic stability metrics are optimised in human gait and therefore are potentially suitable metrics for optimising in an exoskeleton control paradigm.**

## I. INTRODUCTION

In recent years, a large number of lower-limb exoskeletons have been developed to provide assistance to users with lower-limb pathologies [1]. Current exoskeletons are largely used in supervised clinical settings and are not being used to enhance independance in daily life [2]. If exoskeletons are to become widely used devices outside of a clinical setting it is important that a suitable control paradigm is developed that applies the correct assistance that is task and environment specific. Current control paradigms frequently use normalised kinematic trajectories [3], muscle amplification [4], or finite state controllers [5]. The respective issues with these paradigms are that the kinematic trajectory might not be appropriate for the user's task or their environment, the muscle firing patterns may be abnormal, and there are a large number of parameters to tune. There remains a need to develop a control paradigm that works effectively for different tasks and in different enviornments. It is known that the human neuromuscular system optimises energy efficiency and stability [6]. By studying the effect of different walking contexts and constant perturbations (applied via an exoskeleton) on healthy walking, it is posited that there will be an underlying invariant metric that reflects the optimisation of energy efficiency and stability of human gait. This metric can then be optimised as part of an exoskeleton control paradigm enabling asistance to be applied without compromising the stability and energy efficiency of the human gait. Previous work has been carried out to determine what effect walking speed [7]–[9], the environment [10], [11], and exoskeleton forces have [12]–[14] on a user's gait but these are constrained by using limited metrics and for the work done on exoskeletons, limited walking contexts.

In this study, a neuromuscular human and exoskeleton model is presented. Experimental data was collected using a unique setup, combining kinematic, kinetic, and exoskeleton angular and torque data. Using this data, metrics were compared between three walking scenarios: walking without an exoskeleton, walking with an exoskeleton in transparent mode, and walking with an exoskeleton in assistive mode. For each of these scenarios five different walking contexts were investigated: walking at baseline speed, walking up an incline, walking down an incline, fast walking, and slow walking. To carry out the analysis a number of metrics were selected including spatial and temporal parameters, kinematic, kinetic, centre of pressure (CoP), centre of mass (CoM), and other novel dynamic stability metrics. These metrics were then compared to identify the metrics which demonstrated the most invariance and therefore would be suitable for optimising in an exoskeleton control paradigm.

## II. METHODS

### A. Model development

The exoskeleton which we use to provide assistance is the Active Pelvis Orthosis (APO) [15] (see Figure 1(a)) developed by IUVO. The APO provides a force applied to the thighs of the user transmitted via two carbon fibre lateral arms which are actuated by series elastic actuation units.

The APO developers adapted work by Ronsse et al. [16] to construct a high-level assistive controller, which generates a zero-delay estimate of the hip angles during gait and calculates a desired torque which is proportional to the estimated change in hip angle. A constant virtual stiffness parameter is used to calculate the torque necessary to drive the user's joint positions towards their expected future values. The APO can also be operated in 'transparent mode', where the system provides no assistance to the user and the joints are free of resistance.

Our unique model was developed in OpenSIM [17] (see Figure 1(b)) and consists of a human system and the APO. We took a pre-exisiting OpenSIM human model with 92 muscles and 23 DOF [18]–[21] and constrained the APO to it with three weld constraints, located between the backpack and the pelvis and between the two links and the femur. The APO mass and inertia properties were imported from a CAD model.

### B. Experimental protocol

To carry out the experiments approval from the School of Informatic's Ethics Panel was received. Eight participant were recruited to undertake data collection who all gave

G. Henderson, D. Gordon and S. Vijayakumar are with the Department of Informatics, University of Edinburgh, UK. Email: graham.henderson@ed.ac.uk

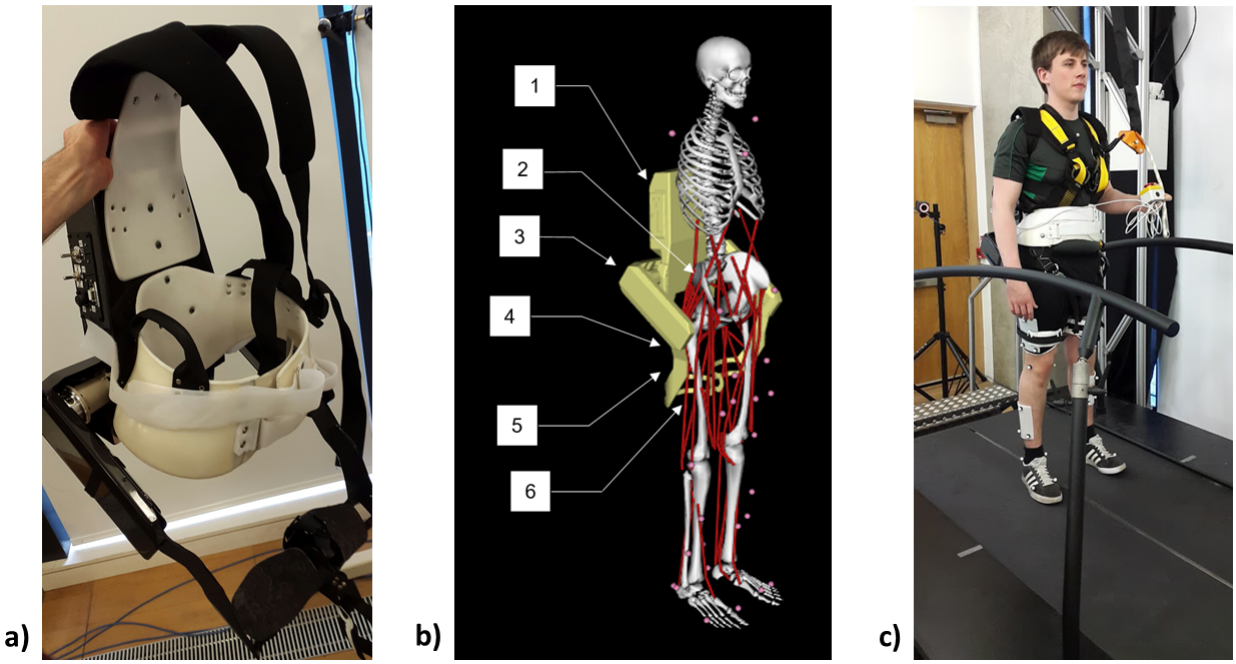


Fig. 1: (a) The Active Pelvis Orthosis (APO) (b) Overview of the APO OpenSIM model's constraints, bodies, and degrees of freedoms (1) APO backpack (2) Weld constraint between APO backpack and pelvis (3) APO group (right) (houses the actuators) (4) APO free joint (6 DOF) (5) APO link (R) (6) Weld constraint between APO right link and right femur (c) the experimental setup

informed consent. Kinematics were collected using a six camera motion capture system (Vicon, Oxford, UK) and ground reaction forces and moments were collected using a six axis, split belt instrumented treadmill (Motekforce Link, Amsterdam, Netherlands) (see Figure 2). The marker set used was adapted from the Cleveland marker set and consisted of 33 markers, 8 of which were solely used for the purpose of scaling the model. Figure 1(c) demonstrates the experimental set up.

To capture data in different contexts we set up a script in the Motek D-Flow software that allowed the subject to walk in 5 different contexts: at baseline walking speed with no incline (BW), at baseline walking speed with an incline of 5°(UW) and with an incline of -5°(DW), at a fast walking speed (FW), and at a slow walking speed (SW). BW was calculated using the principle of dynamic similarity as described by the Froude number [22]:

$$v = \sqrt{F_r \cdot g \cdot L} \tag{1}$$

where $v$ is the baseline speed, $F_r$ is the Froude number (chosen to be 0.1), $g$ is gravitational acceleration ($9.81\text{m/s}^2$), and $L$ is leg length (as measured from the greater trochanter to the medial malleolus). The speeds for FW and SW were calculated by adding and subtracting 20% to the baseline speed respectively. Each context was timed to last 135 seconds, with data collection triggered to happen after 120 seconds to allow for the participant to become accustomed to the context. For time synchronisation, the D-flow script sent a command to a relay box to trigger the Vicon data capture and the APO to record data whilst simultaneously starting to record the kinetic data. The kinematics, ground reaction forces and moments, and APO data were captured at 100Hz, 600Hz, and 100Hz respectively. The contexts were repeated for 3 different assistance scenarios: one without the APO (NE), one with the APO set in transparent mode (ET) and one with the APO set in assistive mode (EA) with the virtual stiffness set to 15Nm/rad.

### C. Post-processing

Before the data could be analysed, several post-processing steps had to be undertaken (see Figure 2). For the kinematic data the MoNMS toolbox [23] was used for the majority of the processing. For the ground reaction forces and moments custom scripts were written in MATLAB. The motion capture data gap filling was undertaken in Vicon's software Nexus. A combination of the built in algorithms were used including the spline fill, the pattern fill, and the cyclic fill.

The kinematic data was then low-pass filtered with a zero-lag 4th order Butterworth filter and transformed from the Vicon axis system into the OpenSIM axis system.

For the ground reaction forces, the first step was to compensate for data collected when the treadmill was tilted and therefore causing gravity to work in a different direction to the forceplate sensors. The ground reaction forces were then filtered using a zero-lag 4th order Butterworth filter with a 6Hz cut-off. For the next step a threshold filter was applied to the ground reaction forces and moments that set all values equal to zero when the vertical force was less than 40N. This was implemented because CoP values are unstable when the vertical ground reaction forces are low. Additionally, it

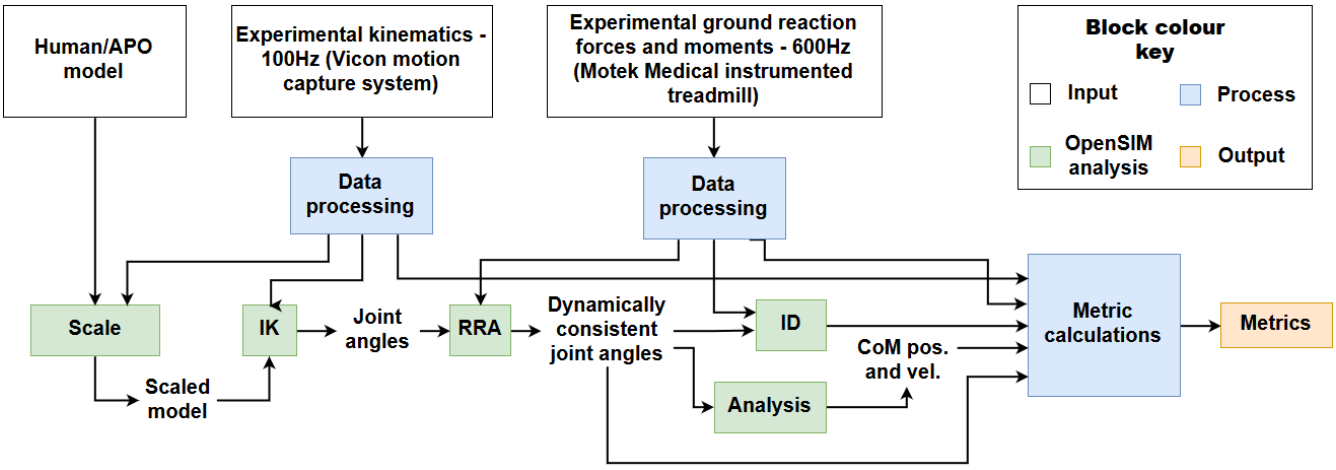


Fig. 2: A schematic demonstrating the data collection and analysis pipeline

| Metric | Dim. | Notation | Unit |
|---|---|---|---|
| Step width | 1 | - | cm |
| Step frequency | 1 | - | steps/min |
| Sagittal hip angles RoM | 1 | $\theta_{\text{hip-RoM}} \in \mathbb{R}^1$ | ° |
| Sagittal peak to peak hip torques | 1 | $\tau_{\text{hip-pp}} \in \mathbb{R}^1$ | Nm/kg |
| CoM displacement | 2 | $\text{CoM}_{\text{disp}} \in \mathbb{R}^2$ | mm |
| CoP displacement | 2 | $\text{CoP}_{\text{disp}} \in \mathbb{R}^2$ | mm |
| Margins of stability | 2 | $\text{MoS} \in \mathbb{R}^2$ | mm |

TABLE I: The metrics' dimensions, notations, and units.

| Subject | Height (m) | Weight (kg) | Walking velocity (m/s) | | |
|---|---|---|---|---|---|
| | | | BW | FW | SW |
| S1 | 1.84 | 76.4 | 0.95 | 1.14 | 0.76 |
| S2 | 1.79 | 67.1 | 0.95 | 1.14 | 0.76 |
| S3 | 1.74 | 58.8 | 0.94 | 1.13 | 0.75 |
| S4 | 1.76 | 77.2 | 0.94 | 1.13 | 0.75 |
| S5 | 1.88 | 83.0 | 0.97 | 1.18 | 0.78 |
| S6 | 1.80 | 61.4 | 0.96 | 1.15 | 0.77 |
| S7 | 1.77 | 66.6 | 0.97 | 1.16 | 0.78 |
| S8 | 1.80 | 75.8 | 0.95 | 1.14 | 0.76 |

TABLE II: The subjects' anthropometric features and walking velocities.

filtered out any noise during the swing phase of the gait cycle when there should be no forces applied to the foot. After applying the threshold, the CoPs were calculated and the global forceplate moments were required to be converted into free moments around the foot. Finally, the D-flow axis system was transformed to the OpenSim axis system.

*Data analysis*

The developed human/APO model was scaled for each subject using 3D marker data at bony landmarks captured during a static pose. The processed data for each subject were divided into 10 gait cycles (5 right and 5 left). Using this processed data in conjunction with the human/APO model and various OpenSIM tools, joint angles were calculated via inverse kinematics and joint torques calculated via inverse dynamics. CoM positions and velocities were calculated via the Analysis tool and the dynamically consistent joint angles via RRA [17] (see Figure 2)). Using these outputs 10 metrics were then calculated (see Table I).

Step width was determined as the medial-lateral distance between the lateral malleolus markers at the heel strikes of consecutive steps.

Step frequency was calculated as the inverse of the time between the heel strikes of consecutive steps.

The hip range of motion ($\theta_{\text{hip-RoM}}$), hip peak to peak torques ($\tau_{\text{hip-pp}}$), and CoM displacements ($\text{CoM}_{\text{disp}}$) were calculated by subtracting their respective maximum values from their minimum values over the gait cycle. For the CoP displacement ( $\text{CoP}_{\text{disp}}$), this was calculated as the maximum value minus the minimum value over the stance phase period.

The margins of stability MoS were calculated as specified by Hof [24]:

$$MoS = \left| u_{max} - (x + \frac{v}{\omega_0}) \right| \tag{2}$$

where $u_{max}$ is the boundary of the base of support, $x$ is the centre of mass position, $v$ is the centre of mass velocity, and $\omega_0$ is equal to:

$$\omega_0 = \sqrt{\frac{g}{l}} \tag{3}$$

where $g$ is the acceleration of gravity and $l$ is the distance from the pelvis ASIS to the lateral malleolus.

*D. Statistical analysis*

To investigate the effects of the exoskeleton assistance and the walking context on the metrics, a two-way ANOVA was used. For the post-hoc analysis, the MATLAB multiple comparison procedure 'multcompare' was used with the comparison type based on Tukey's honestly significant difference criterion. The statistical significance level was set at $\alpha = 0.05$.

For pairs of context and assistance scenarios which demonstrated a significant difference in the mean of a metric, the effect size was measured by computing the absolute value[1] of Cohen's $d$. These values were then averaged to produce a quantitative measure of invariance for each metric

[1]The decision to take the absolute value was motivated by an interest in the magnitude of an effect rather than it's direction.

| Quantity | Value | OpenSIM Benchmark |
|---|---|---|
| RMS Residual force (N) | $7.1 \pm 3.4$ | $< 10$ |
| Peak Residual force (N) | $17.9 \pm 7.6$ | $< 25$ |
| RMS Residual moment (N) | $7.3 \pm 4.0$ | $< 50$ |
| Peak Residual moment (N) | $16.9 \pm 8.7$ | $< 75$ |

TABLE III: RRA residuals in OpenSim.

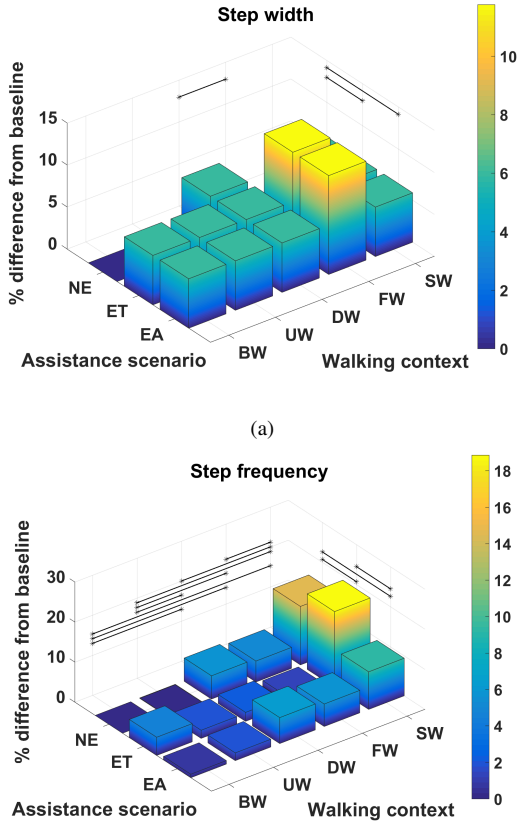


(a)

(b)

Fig. 3: (a) Step width and (b) step frequency percentage difference from baseline, categorised by walking context and assistance scenario. Black lines represent significant differences.

relative to changes in assistance level, changes in walking context, and overall.

## III. RESULTS

The anthropometric measurements and calculated walking velocities for each subject are presented in Table II.

Running the RRA tool for all the data sets generated RMS and peak residuals for FX, FY, FZ, MX, MY, and MZ. All the average forces were less than the thresholds specified by the OpenSIM developers (see Table III).

For each metric and for every context and assistance scenario the percentage difference from the baseline condition (no exoskeleton assistance and walking at baseline speed) is demonstrated in Figures 3-7. Additionally, the mean and standard deviation values for every context and assistance scenario combination are detailed in the Table IV.

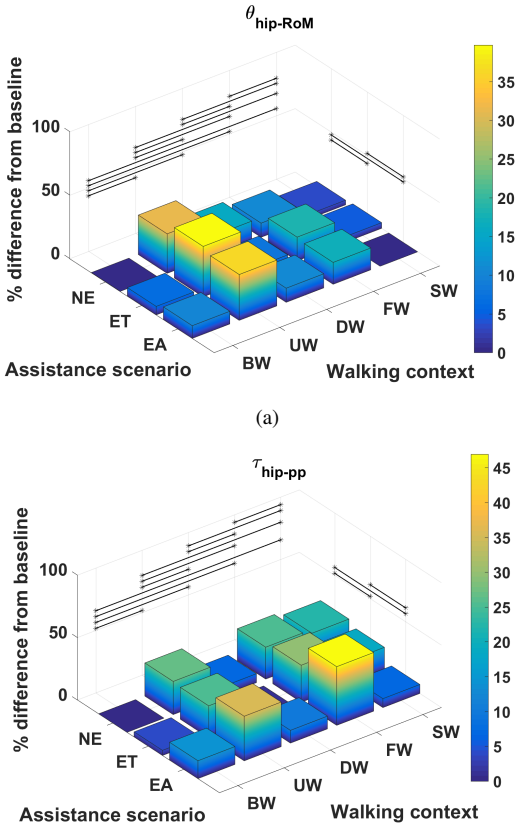


(a)

(b)

Fig. 4: (a) $\theta_{\text{hip-RoM}}$ and (b) $\tau_{\text{hip-pp}}$ percentage difference from baseline, categorised by walking context and assistance scenario. Black lines represent significant differences

*Invariance over contexts*

By undertaking ANOVA for each metric, the pairs of contexts with significant different means were calculated and are displayed in Figures 3-7. By comparing between metrics, it is demonstrated that step width, CoP-ML$_{\text{disp}}$, and MoS-ML$_{\text{disp}}$ are the most invariant in terms of the numbers of significant differences. When considering the effect sizes (see Figure 8), the same three metrics also demonstrate Cohen's d values that indicate between small (d = 0.2) and medium (d = 0.5) effect sizes. All of the other metrics show effect sizes of greater than medium.

*Invariance over assistance scenarios*

Similarly to the contexts, the pairs of assistance scenarios with significant different means were calculated (see Figures 3-7). The metrics with the most invariance by number of significant differences are the CoP-AP$_{\text{disp}}$ and similarly to the context results, the MoS-ML. After factoring in the effect sizes (see Figure 9) the same two metrics and in addition the CoM-ML$_{\text{disp}}$ and MoS-AP metrics demonstrate Cohen's d values that indicate between very small (d = 0.1) and small effect sizes. The other metrics demonstrate effect sizes of between small and medium.

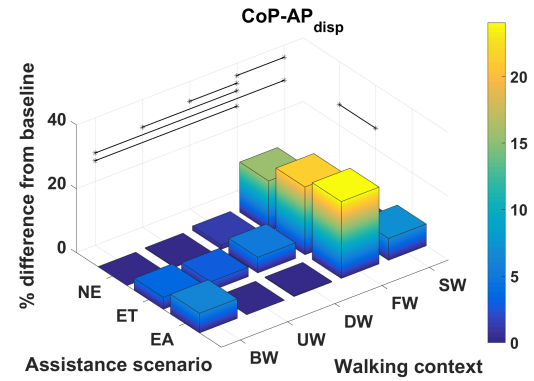


(a)

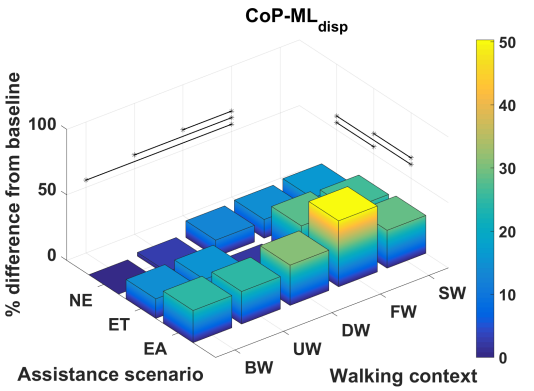


(b)

Fig. 5: (a) CoP-$AP_{disp}$ and (b) CoP-$ML_{disp}$ percentage difference from baseline, categorised by walking context and assistance scenario. Black lines represent significant differences.

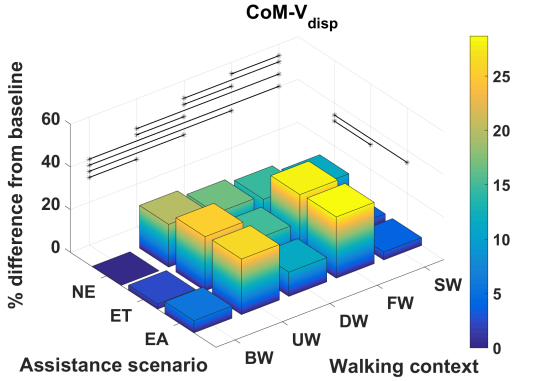


(a)

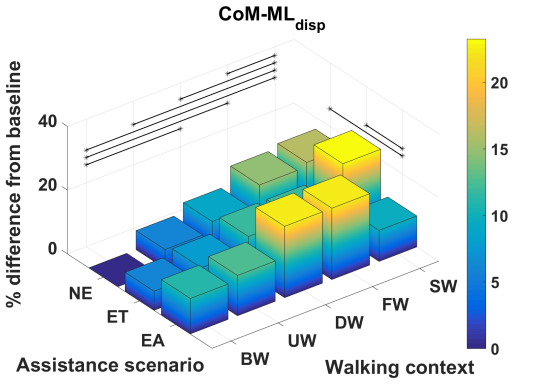


(b)

Fig. 6: (a) CoM-$V_{disp}$ and (b) CoM-$ML_{disp}$ percentage difference from baseline, categorised by walking context and assistance scenario. Black lines represent significant differences.

*Summary*

Figures 3-7 demonstrate that step width and MoS-ML are the most overall invariant metrics with 3 and 4 significant different pairs of means respectively. In Figure 10 are the average effect sizes for each of the metrics. For step width, CoP-$ML_{disp}$, and MoS-ML the Cohen's d values were between 0.2 and 0.5, which is an effect sizes of small to medium. The small effect size for the CoP-$ML_{disp}$ significant differences suggest that it is also an invariant metric.

## IV. DISCUSSION AND FURTHER WORK

It is well known that walking speed is a cause of gait variability for kinematic, kinetic, and $CoM_{disp}$ metrics [7]–[9] and the results from this study also demonstrate the same findings. This study demonstrates that step frequency increases due to speed and anecdotally suggests that step length increases as well (step length was not included in the analysis due to unavailability of complete consecutive step data for some of the participants due to cross-talk on the force plates). The step width was demonstrated to be invariant with only one significant difference with a small effect size between walking downhill and walking at a fast speed. Walking speed causes variation for the CoP-$AP_{disp}$ and the CoP-$ML_{disp}$ metrics, however, the effect on the CoP-$ML_{disp}$ is small and only between the fast and baseline walking speed contexts. In addition, walking speed affects the MoS-AP and MoS-ML, similarly to the $CoP_{disp}$ there is only a small effect in the medial lateral direction between the slow and baseline walking speed contexts. It is a logical result that walking speed has a greater effect on the metrics measured in the anterior posterior direction compared to the medial lateral direction because walking speed is a change of direction mainly in the anterior posterior direction.

The effect of walking up and down an incline, similarly to speed has previously been demonstrated to have significant kinematic and kinetic changes [10] and the results from this study support this result. In additional to the effects on kinematics and kinetics the results from this study indicate that walking on an incline affects the CoM-$V_{disp}$ and that walking down an incline affects the step frequency, the CoM-$V_{disp}$, the CoM-$ML_{disp}$, and the MoS-AP. The increase in step frequency is expected due to a shorter step length being taken. The effects on the CoM vertical displacement are also expected due to the change in height caused by the slope. The effect on the MoS-AP are expected because this measures the stability in the backwards direction and it is clear that when the torso is tilted forwards then the MoS-AP values will increase. Neither walking up or down an incline had any effect on the MoS-ML.

This study demonstrates there are significant differences

| AS | Step width (cm) | | | | | Step frequency (steps/min) | | | | |
|---|---|---|---|---|---|---|---|---|---|---|
| | BW | UW | DW | FW | SW | BW | UW | DW | FW | SW |
| NE | 17 ± 4 | 17 ± 3 | 18 ± 5 | 17 ± 4 | 16 ± 4 | 103.4 ± 8.7 | 103.5 ± 9.8 | 109.4 ± 9.0 | 108.8 ± 8.5 | 88.3 ± 6.7 |
| ET | 16 ± 4 | 16 ± 2 | 16 ± 3 | 15 ± 4 | 16 ± 3 | 98.7 ± 14.8 | 101.3 ± 6.9 | 105.7 ± 6.5 | 104.9 ± 12.3 | 83.9 ± 8.8 |
| EA | 16 ± 3 | 16 ± 3 | 16 ± 3 | 15 ± 4 | 16 ± 4 | 104.3 ± 5.3 | 105.4 ± 6.7 | 110.1 ± 6.9 | 109.2 ± 12.9 | 93.7 ± 7.5 |
| AS | $\theta_{\text{hip-RoM}}$(Sagittal hip angles RoM (°)) | | | | | $\tau_{\text{hip-pp}}$(Sagittal peak to peak hip torques (Nm/kg)) | | | | |
| | BW | UW | DW | FW | SW | BW | UW | DW | FW | SW |
| NE | 36.0 ± 3.0 | 47.2 ± 3.8 | 30.4 ± 3.6 | 40.0 ± 3.2 | 34.7 ± 3.7 | 0.98 ± 0.2 | 1.24 ± 0.2 | 0.91 ± 0.2 | 1.23 ± 0.2 | 0.76 ± 0.2 |
| ET | 38.4 ± 2.7 | 50.3 ± 2.7 | 33.3 ± 3.8 | 42.7 ± 2.8 | 37.6 ± 3.5 | 1.02 ± 0.2 | 1.23 ± 0.2 | 0.97 ± 0.1 | 1.27 ± 0.1 | 0.80 ± 0.2 |
| EA | 39.6 ± 3.6 | 49.0 ± 3.0 | 32.0 ± 3.2 | 42.2 ± 3.1 | 36.0 ± 5.2 | 1.12 ± 0.1 | 1.33 ± 0.1 | 1.08 ± 0.2 | 1.44 ± 0.3 | 0.91 ± 0.2 |
| AS | CoP-AP$_{\text{disp}}$(CoP anterior posterior displacement (mm)) | | | | | CoP-ML$_{\text{disp}}$(CoP medial lateral displacement (mm)) | | | | |
| | BW | UW | DW | FW | SW | BW | UW | DW | FW | SW |
| NE | 419.1 ± 52.2 | 420.2 ± 56.8 | 413.4 ± 57.7 | 484.9 ± 83.7 | 403.3 ± 50.3 | 32.2 ± 14.6 | 31.3 ± 9.6 | 28.1 ± 13.6 | 36.8 ± 16.8 | 37.5 ± 20.3 |
| ET | 434.7 ± 45.8 | 431.3 ± 46.7 | 439.6 ± 81.8 | 508.0 ± 51.6 | 427.5 ± 49.2 | 37.0 ± 16.5 | 37.2 ± 13.8 | 31.5 ± 14.9 | 41.2 ± 16.9 | 40.7 ± 28.5 |
| EA | 444.9 ± 65.4 | 419.2 ± 55.1 | 418.1 ± 79.9 | 519.9 ± 101.5 | 390.5 ± 51.4 | 40.1 ± 18.2 | 40.2 ± 14.8 | 42.1 ± 18.2 | 48.4 ± 24.2 | 41.5 ± 18.4 |
| AS | CoM-V$_{\text{disp}}$(CoM vertical displacement (mm)) | | | | | CoM-ML$_{\text{disp}}$(CoM medial lateral displacement (mm)) | | | | |
| | BW | UW | DW | FW | SW | BW | UW | DW | FW | SW |
| NE | 30.0 ± 4.9 | 36.0 ± 6.0 | 35.0 ± 6.0 | 34.4 ± 4.0 | 26.6 ± 4.1 | 58.5 ± 19.7 | 55.0 ± 13.6 | 53.2 ± 19.3 | 49.8 ± 17.6 | 68.0 ± 23.2 |
| ET | 30.7 ± 4.8 | 37.6 ± 4.7 | 34.5 ± 5.9 | 38.4 ± 5.8 | 28.9 ± 5.1 | 55.0 ± 18.8 | 54.0 ± 12.2 | 51.6 ± 16.7 | 51.6 ± 16.0 | 72.1 ± 18.5 |
| EA | 31.7 ± 4.1 | 37.8 ± 5.0 | 33.4 ± 4.6 | 38.6 ± 5.7 | 28.9 ± 4.0 | 52.0 ± 13.7 | 51.1 ± 12.2 | 45.4 ± 14.3 | 45.4 ± 12.6 | 64.2 ± 18.7 |
| AS | MoS-AP (Margins of stability - anterior posterior (mm)) | | | | | MOS-ML (Margins of stability - medial lateral (mm)) | | | | |
| | BW | UW | DW | FW | SW | BW | UW | DW | FW | SW |
| NE | 104.0 ± 36.1 | 101.8 ± 46.9 | 157.8 ± 45.4 | 120.8 ± 46.1 | 59.3 ± 36.3 | 68.8 ± 16.9 | 70.2 ± 18.6 | 72.05 ± 17.4 | 69.5 ± 20.6 | 63.3 ± 21.7 |
| ET | 90.2 ± 34.8 | 102.3 ± 39.6 | 135.6 ± 32.6 | 112.3 ± 25.6 | 39.8 ± 30.8 | 71.8 ± 17.3 | 70.1 ± 17.2 | 66.16 ± 15.3 | 71.75 ± 18.6 | 62.2 ± 18.6 |
| EA | 97.5 ± 25.7 | 112.5 ± 40.8 | 144.5 ± 41.9 | 125.5 ± 36.5 | 64.4 ± 30.1 | 68.7 ± 18.7 | 69.4 ± 15.8 | 70.0 ± 21.4 | 70.3 ± 18.5 | 66.8 ± 16.2 |

TABLE IV: mean ±SD of metrics categorised by walking context and assistance scenario.

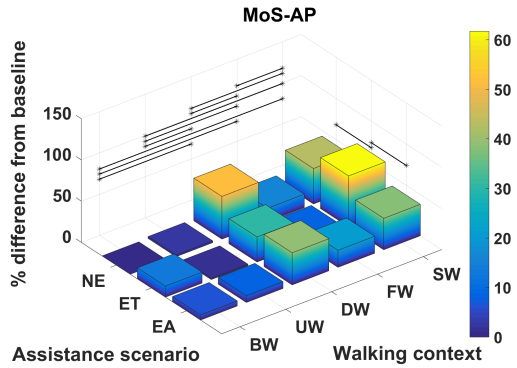


(a)

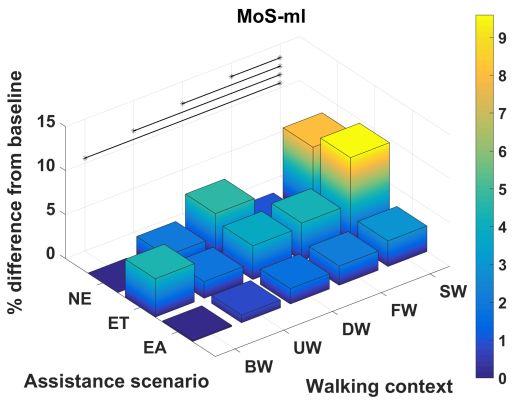


(b)

Fig. 7: (a) MoS-AP and (b) MoS-ML percentage difference from baseline, categorised by walking context and assistance scenario. Black lines represent significant differences.

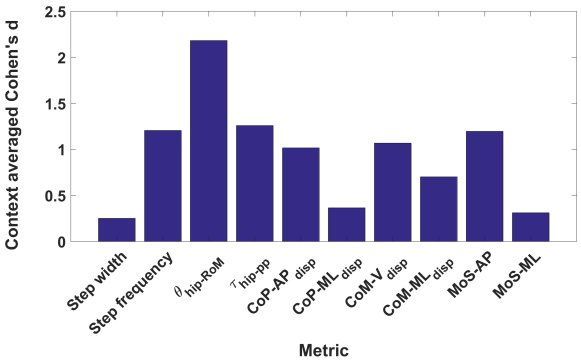


Fig. 8: The context average effect sizes.

between the $\theta_{\text{hip-RoM}}$ caused by context and assistance scenario changes. This result aligns with the work by d'Elia et al. [25], and similarly their claim that the differences between the assistance scenario $\theta_{\text{hip-RoM}}$s are within natural varation of gait is also applicable. There was a significant increase in the $\tau_{\text{hip-pp}}$ from the ET to the EA scenario. This result suggests a disagreement with a study by Lewis and Ferris [14], which found that the net torques did not change between walking with an exoskeleton in passive mode and with it in assistive mode. The result from our study suggests that torque from the exoskeleton is not entirely being transferred to the individual, which is quite probable due to the non-rigid attachments of the exoskeleton. There is a significant increase in the CoP-ML$_{\text{disp}}$ from the NE and the ET and EA scenarios, which can be attributed to the extra weight of the exoskeleton laterally located to the participant. One consideration for the above findings is that the effect sizes for all the metrics for the assistance scenarios were between small and medium, which suggests the differences are small between the assistance scenarios. This is in contrast to the

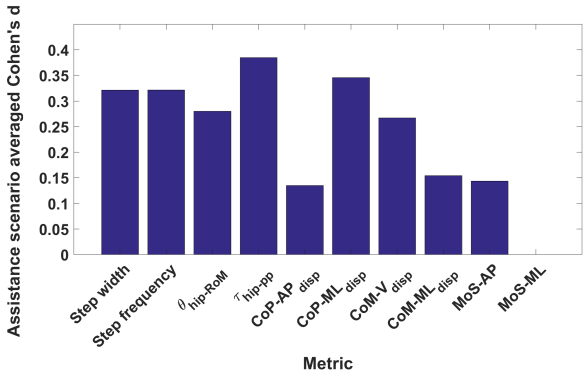


Fig. 9: The assistance scenario average effect sizes.

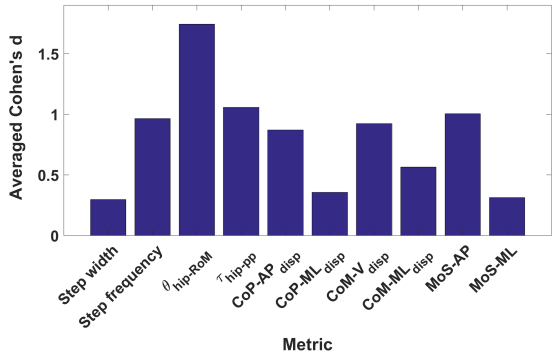


Fig. 10: The overall average effect sizes.

context effect sizes, where 6 out of the 10 metrics had large or greater effect sizes.

All the metrics demonstrated some significant differences due to the changes in walking context and assistance scenario. After factoring in the effect sizes the most invariant metrics were shown to be the step width, the CoP-$ML_{disp}$, and the MoS-ML. All three metrics have been demonstrated to be associated with stability [6], [24], and [26] therefore it is intuitive that they remain fairly constant despite changes in walking context and the application of small constant perturbations. The CoP and MoS metrics are more suitable for use in a control paradigm because they can be calculated at any given time during a gait cycle and therefore enable a significantly more responsive controller. To determine which metric should be implemented in a control paradigm it is important to study the invariance of the metrics over a gait cycle and the changes in the metric between healthy individuals and those with gait pathologies.

## ACKNOWLEDGMENT

This research is supported by the Engineering and Physical Sciences Research Council (EPSRC), as part of the CDT in Robotics and Autonomous Systems at Heriot-Watt University and the University of Edinburgh.

## REFERENCES

[1] A. M. Dollar and H. Herr, "Lower extremity exoskeletons and active orthoses: challenges and state-of-the-art," *IEEE Transactions on robotics*, vol. 24, no. 1, pp. 144–158 2008.

[2] J. Wolff *et al.*, "A survey of stakeholder perspectives on exoskeleton technology," *J Neuroeng Rehabil*, vol. 11 2014.

[3] R. Riener *et al.*, "Locomotor training in subjects with sensori-motor deficits: an overview of the robotic gait orthosis lokomat," *Journal of Healthcare Engineering*, vol. 1, no. 2, pp. 197–216 2010.

[4] D. P. Ferris and C. L. Lewis, "Robotic Lower Limb Exoskeletons Using Proportional Myoelectric Control," *Conf Proc IEEE Eng Med Biol Soc*, vol. 2009, pp. 2119–2124 2009.

[5] J. A. Blaya and H. Herr, "Adaptive control of a variable-impedance ankle-foot orthosis to assist drop-foot gait," *IEEE Trans Neural Syst Rehabil Eng*, vol. 12, no. 1, pp. 24–31 2004.

[6] A. D. Kuo and J. M. Donelan, "Dynamic Principles of Gait and Their Clinical Implications," *Phys Ther*, vol. 90, no. 2, pp. 157–174 2010.

[7] D. A. Winter, "Kinematic and kinetic patterns in human gait: Variability and compensating effects," *Human Movement Science*, vol. 3, no. 12, pp. 51–76 1984.

[8] B. W. Stansfield *et al.*, "Sagittal joint kinematics, moments, and powers are predominantly characterized by speed of progression, not age, in normal children," *J Pediatr Orthop*, vol. 21, no. 3, pp. 403–411 2001.

[9] M. S. Orendurff *et al.*, "The effect of walking speed on center of mass displacement," *J Rehabil Res Dev*, vol. 41, no. 6A, pp. 829–834 2004.

[10] A. N. Lay, C. J. Hass, and R. J. Gregor, "The effects of sloped surfaces on locomotion: A kinematic and kinetic analysis," *Journal of Biomechanics*, vol. 39, no. 9, pp. 1621–1628 2006.

[11] J. R. Franz and R. Kram, "The Effects of Grade and Speed on Leg Muscle Activations during Walking," *Gait Posture*, vol. 35, no. 1, pp. 143–147 2012.

[12] T. Lenzi *et al.*, "Reducing muscle effort in walking through powered exoskeletons," *Conf Proc IEEE Eng Med Biol Soc*, vol. 2012, pp. 3926–3929 2012.

[13] D. Martelli *et al.*, "The effects on biomechanics of walking and balance recovery in a novel pelvis exoskeleton during zero-torque control," *Robotica*, vol. 32, no. 08, pp. 1317–1330 2014.

[14] C. L. Lewis and D. P. Ferris, "Invariant hip moment pattern while walking with a robotic hip exoskeleton," *J Biomech*, vol. 44, no. 5, pp. 789–793 2011.

[15] F. Giovacchini *et al.*, "A light-weight active orthosis for hip movement assistance," *Robotics and Autonomous Systems*, vol. 73, pp. 123–134 2015.

[16] R. Ronsse *et al.*, "Oscillator-based assistance of cyclical movements: model-based and model-free approaches," *Med Biol Eng Comput*, vol. 49, no. 10, p. 1173 2011.

[17] S. L. Delp *et al.*, "OpenSim: open-source software to create and analyze dynamic simulations of movement," *IEEE Trans Biomed Eng*, vol. 54, no. 11, pp. 1940–1950 2007.

[18] ——, "An interactive graphics-based model of the lower extremity to study orthopaedic surgical procedures," *IEEE Trans Biomed Eng*, vol. 37, no. 8, pp. 757–767 1990.

[19] G. T. Yamaguchi and F. E. Zajac, "A planar model of the knee joint to characterize the knee extensor mechanism," *J Biomech*, vol. 22, no. 1, pp. 1–10 1989.

[20] F. C. Anderson and M. G. Pandy, "A Dynamic Optimization Solution for Vertical Jumping in Three Dimensions," *Comput Methods Biomech Biomed Engin*, vol. 2, no. 3, pp. 201–231 1999.

[21] ——, "Dynamic optimization of human walking," *J Biomech Eng*, vol. 123, no. 5, pp. 381–390 2001.

[22] C. L. Vaughan and M. J. O'Malley, "Froude and the contribution of naval architecture to our understanding of bipedal locomotion," *Gait Posture*, vol. 21, no. 3, pp. 350–362 2005.

[23] A. Mantoan *et al.*, "MOtoNMS: A MATLAB toolbox to process motion data for neuromusculoskeletal modeling and simulation," *Source Code for Biology and Medicine*, vol. 10, p. 12 2015.

[24] A. L. Hof, M. G. J. Gazendam, and W. E. Sinke, "The condition for dynamic stability," *Journal of Biomechanics*, vol. 38, no. 1, pp. 1–8 2005.

[25] N. dElia *et al.*, "Physical human-robot interaction of an active pelvis orthosis: toward ergonomic assessment of wearable robots," *Journal of NeuroEngineering and Rehabilitation*, vol. 14, p. 29 2017.

[26] Z. Svoboda *et al.*, "Variability of centre of pressure displacements during gait in fallers and nonfallers: A 6-month prospective study," *Gait & Posture*, vol. 49, p. 160 2016.